ISSN: 2754-6705

Journal of Mathematical & Computer Applications

SCIENTIFIC Research and Community

Review Article

Open Access

Computational Approach in Mathematical Modeling of Cell Mass Concentration Effect on Heat Transfer Through a Blood Channel

KW Bunonyo[1*], AB Moko[2] and Tamuno Boma Odinga[3]

[1]MMDARG, Department of Mathematics and Statistics, Federal University Otuoke, Nigeria

[2]Department of Computer Science and Informatics, Federal University Otuoke, Nigeria

[3]Department of Biochemistry, Rivers State University, Nigeria

ABSTRACT

This study involves a mathematical formulation of models representing the cell-induced mass concentration effect on heat transfer through a blood channel with the aim of understanding the role mass concentration plays on blood circulation. The models were derived as partial differential equations in dimensional form, scaled, and reduced to ordinary differential equations. The direct method of solving differential equations was adopted, and profiles were used. and the ODEs for the temperature and concentration profiles were obtained, respectively. In order to investigate the impact of the cell mass concentration effect on the heat transfer through the blood channel, we carried out a numerical simulation using Wolfram Mathematica, where the pertinent parameters such as the Prandtl number, Schmidt number, oscillatory parameter, radiation parameter, and mass concentration parameter on the flow profiles were used. In conclusion, the results suggested that the fluid temperature could increase with heat source, concentration rate, and Prandtl number, but decreases with oscillatory effects. Secondly, concentration decreases with increasing reaction rate, oscillation, and Schmidt number.

***Corresponding author**

KW Bunonyo, MMDARG, Department of Mathematics and Statistics, Federal University Otuoke, Nigeria.

Received: February 14, 2026; **Accepted:** February 19, 2026, **Published:** February 27, 2026

Keywords: MMDARG, Sickle Cell, Blood, Bioheat, Mass Concentration, Mathematical Modelling, Channel

Nomenclature

y^*	Dimensional vertical distance
C^*	Dimensional cell mass concentration
T^*	Dimensional temperature
C_∞	Far field cell mass concentration
T_∞	Far field temperature
Q_0	Heat source due to temperature
Q_1	Cell mass concentration source
	Blood density
c_{bp}	Blood specific heat capacity
k_{bT}	Blood thermal conductivity
D_m	Mass diffusivity
k_0	Chemical reaction
k_T	Lipid concentration treatment
t^*	Dimensional time
Rd_1	Heat source term
Rd_2	Cell mass concentration source term
Rd_3	Chemical reaction term
ϕ	Dimensionless cell mass concentration
θ	Dimensionless temperature
Pr	Prandtl number
Sc	Schmidt number

Introduction

Blood is a specialized fluid tissue in the human body that plays a pivotal role in sustaining life. It performs critical functions including oxygen transport, immune defense, hormone distribution, and waste removal. The composition of blood includes plasma, red blood cells (RBCs), white blood cells (WBCs), and platelets. Blood is an electrolytic fluid composed of ions, proteins, and cells, allowing it to conduct electrical signals. The presence of red blood cells (RBCs) in the blood volume such as sickle and normal cells affects the dielectric properties and conductivity of blood. These factors are crucial in bio-impedance studies and biosensor applications. Red blood cells, RBCs exhibit deformability and consistent shape, contributing to uniform conductivity, and sickle RBCs are rigid and irregular, leading to alteration of flow channel, dynamics and electrical impedance. conducted a study on anatomy, blood flow. In this study a mathematical model was formulated to investigate the flow of blood on the human vessels and organs through which blood flow in the body [1]. Blood consists of two main components, namely, plasma (55%), the liquid portion of blood that contains water, electrolytes, proteins (such as albumin and fibrinogen), glucose, lipids, hormones, and waste products like urea. It serves as a medium for transporting cells and substances throughout the body. Bunonyo et al. conducted a study on the lipid

concentration effects of blood flow through an inclined arterial channel with magnetic field. Red Blood Cells are cells responsible for carrying oxygen from the lungs to tissues and transporting carbon dioxide back to the lungs for exhalation. RBCs contain haemoglobin, a protein that binds to oxygen and facilitates gas exchange, while White Blood Cells are part of the immune system and protect the body against infections and foreign substances. WBCs include neutrophils, lymphocytes, monocytes, eosinophils, and basophils.

Red blood cells, also called erythrocytes, are the most abundant type of blood cell; Red blood cells have a lifespan of about 120 days and are constantly being replaced by new cells. Red blood cell membrane-derived cholesterol as a trigger for lipid core expansion and inflammation, and the casual relationship between elevated cholesterol level and atherosclerosis is known for more than 60 years. Early atherosclerotic lesions are characterized by subendothelial accumulation of cholesterol-laden macrophages called foam-cells. During plaque progression foam cells dye and release free cholesterol that deposits inside the plaque forming the necrotic core a characteristic feature of more advanced lesions (Lusis, 2000). For decades low-density lipoprotein (LDL) was considered as the main source of atherosclerotic plaque lipid content, and lowering circulating LDL-cholesterol level is still a major approach for anti-atherosclerotic therapies [2]. For example, it has been shown that familial hypercholesterolemia is associated with elevated RBC membrane-associated cholesterol and that high-fat diet increase membrane lipid content of RBCs in experimental animal models [3]. Accordingly, lipid lowering strategies such as statin treatment and life-style changes have been shown to positively modulate RBC lipid composition which might contribute to the atheroprotective effects of these approaches [4].

Sickle cell disease (SCD) is a genetic blood disorder characterized by the production of abnormal haemoglobin (HbS), which distorts red blood cells into a sickle or crescent shape. These distorted cells affect blood flow and oxygen delivery, contributing to various complications. Recent biomedical research has explored the electrochemical and piezoelectric properties of biological systems to understand the electrical signals generated by cellular activity.

Sickle cell disease (SCD) has also been shown to be associated with a very high rate (50 to 90%) of childhood mortality [5]. Sickle cell anemia, the first genetic disease to be described in terms of a gene mutation, is one of the most common genetic causes of illness and death in the world [6].

Sickle cell is a red blood cell that has an abnormal crescent or sickle shape due to a mutation in the haemoglobin gene (HbS). These cells are less flexible and can block blood flow in small vessels, leading to pain and tissue damage [7]. The proportion or number of sickle red blood cells in a given volume of blood is called the concentration of sickle cell. It is used to assess the severity or progression of sickle cell disease [8]. However, in this research we are going to formulate mathematical model that represent the impact of sickle cell mass concentration on heat transfer through the blood vessel.

Mathematical Formulation

For us to investigate the impact of packed cell mass concentration energy transfer through the blood channel, we shall consider the following assumptions:

Assumptions

The assumptions are:

- The boundary layer formation is caused by packed cell concentration
- The energy transfer is affected by heat source
- The energy transfer is affected by the packed cell mass concentration
- The packed cell concentration is affected by chemical reaction and fixed treatment on the cell concentration.

Following the above assumptions and Bunonyo et al. we shall present the models representing the system as [9-11]:

Energy Equation with Heat Source

$$\rho_b c_{bp} \frac{\partial T^*}{\partial t^*} = k_{bT} \frac{\partial^2 T^*}{\partial y^{*2}} + Q_0 \left(T^* - T_\infty\right) + Q_1 \left(C^* - C_\infty\right) \tag{3.1}$$

Cell Mass Concentration Equation with Treatment

$$\frac{\partial C^*}{\partial t^*} = D_m \frac{\partial^2 C^*}{\partial y^{*2}} - k_0 k_T \left(C^* - C_\infty\right) \tag{3.2}$$

The Corresponding Boundary Conditions are:

$$\left.\begin{aligned} T^* = 0, C^* = 0 \quad \text{at } y^* = 0 \\ T^* = T_w, C^* = C_w \text{ at } y^* = R_0 \end{aligned}\right\} \tag{3.3}$$

The boundary formed as a result of the packed cell mass can be modeled to be:

$$y^* = \begin{cases} R_0 & \text{at } 0 \le x^* \le d_0 \\ R_1 + \delta_1^* e^{a_1 t} \cos\left(\dfrac{2\pi x^*}{\lambda_1}\right) & \text{at } d_0 \le x^* \le \lambda_1 \\ R_2 + \delta_2^* e^{a_2 t} \cos\left(\dfrac{2\pi x^*}{\lambda_2}\right) & \text{at } \lambda_1 \le x^* \le d_2 \\ R_1 + R_2 + \delta_1^* e^{a_1 t} \cos\left(\dfrac{2\pi x^*}{\lambda_1}\right) + \delta_2^* e^{a_2 t} \cos\left(\dfrac{2\pi x^*}{\lambda_2}\right) & \text{at } d_2 \le x^* \le \lambda_2 \end{cases} \tag{3.4}$$

We introduce the following non-dimensional quantities to make the governing equations dimensionless; they are as follows:

$$\left.\begin{aligned} &\theta = \frac{T^* - T_\infty}{T_w - T_\infty}, \phi = \frac{C^* - C_\infty}{C_w - C_\infty}, Gr = \frac{g\beta_T \left(T_w - T_\infty\right) R_0^3}{\upsilon^2}, Gc = \frac{g\beta_C \left(C_w - C_\infty\right) R_0^3}{\upsilon^2}, Rd_3 = \frac{k_0 R_0^2}{\upsilon}, \\ &Rd_2 = \frac{Q_1 \left(C^* - C_\infty\right) R_0^2}{k_T \left(T_w - T_\infty\right)}, M = B_0 R_0 \sqrt{\frac{\sigma_e}{\mu_b}}, x = \frac{x^*}{\lambda}, y = \frac{y^*}{R_0}, w = \frac{w^* R_0}{\upsilon}, t = \frac{\upsilon t^*}{R_0^2}, \delta_1^* = \delta_1 R_0, \\ &\delta_2^* = \delta_2 R_0, \frac{1}{k} = \frac{\varphi R_0^2}{k^*}, Pr = \frac{\mu_b c_b}{k_{Tb}}, Rd_1 = \frac{Q_0 R_0^2}{\mu_b c_b}, Sc = \frac{\upsilon}{D_m}, h_1 = \frac{R_1}{R_0}, h_2 = \frac{R_2}{R_0}, x = \frac{x^*}{\lambda_1}, x = \frac{x^*}{\lambda_2} \end{aligned}\right\} \tag{3.5}$$

Using equation (3.6) on the governing equations (3.1) - (3.5), the governing equations are reduced to the following dimensionless equations governing the flow, which are:

$$Pr \frac{\partial \theta}{\partial t} = \frac{\partial^2 \theta}{\partial y^2} + \theta k_T Pr Rd_1 + \phi Rd_2 \tag{3.6}$$

$$\frac{\partial \phi}{\partial t} = \frac{1}{Sc}\frac{\partial^2 \phi}{\partial y^2} - Rd_3\phi \tag{3.7}$$

Using the conditions in equation (3.6) in simplifying equation (3.5), the atherosclerotic boundaries, we have:

$$y = \begin{cases} 1 & \text{at } \ 0 \le x \le \frac{d_0}{\lambda} \\ h_\alpha = h_1 + \delta_1 e^{a_1 t}\cos(2\pi x_1) & \text{at } \ \frac{d_0}{\lambda_1} \le x \le 1 \\ h_\beta = h_2 + \delta_2 e^{a_2 t}\cos(2\pi x_2) & \text{at } \ 1 \le x \le \frac{d_2}{\lambda_2} \\ h_\gamma = (h_1 + h_2) + (\delta_1 e^{a_1 t} + \delta_2 e^{a_2 t})\cos(2\pi x) & \text{at } \ \frac{d_2}{\lambda_2} \le x \le 1 \end{cases} \tag{3.8}$$

The corresponding atherosclerotic boundary conditions derived from equation (3.10a), we have:

$$\left.\begin{array}{l} \theta = 0, \phi = 0, \text{ at } \ y = 0 \\ \theta = 1, \phi = 1, \ \text{ at } \ y = h_\alpha \end{array}\right\} \tag{3.9}$$

Perturbation of the System

We shall adopt the oscillatory perturbation method by considering that the flow caused by the pumping action of the heart. Hence, we considered the flow profiles to be in the form according to [12]:

$$\left.\begin{array}{l} \theta = \theta_0 e^{\omega t} \\ \phi = \phi_0 e^{\omega t} \end{array}\right\} \tag{3.10}$$

Substituting equation (3.12) into equations (3.7) - (3.9), we have:

$$\frac{d^2\theta_0}{dy^2} + \beta_2^2\theta_0 = -\phi_0 Rd_2 \tag{3.11}$$

$$\frac{d^2\phi_0}{dy^2} - \beta_3^2\phi_0 = 0 \tag{3.12}$$

where $\beta_2^2 = Pr(Rd_1 - \omega)$, and $\beta_3^2 = (Rd_3 + \omega)Sc$

The boundary conditions are:

$$\left.\begin{array}{ll} \theta_0 = 0, \phi_0 = 0, & \text{at } \ y = 0 \\ \theta_0 = e^{-\omega t} = \theta_a, \phi_0 = e^{-\omega t} = \phi_a, & \text{at } \ y = h_\alpha \end{array}\right\} \tag{3.13}$$

Solving equation (3.12), we have:

$$\phi_0 = c_1 sinh\beta_3 y + c_2 cosh\beta_3 y \tag{3.14}$$

Solving equation (3.14) using the boundary conditions in equation (3.13), we have:

$$\phi_0 = c_1 sinh\beta_3 y \tag{3.15}$$

where $c_1 = \dfrac{e^{-\omega t}}{sinh\beta_3 h_\alpha}$

Simplifying equation (3.15) using the normal boundary conditions, we have:

$$\phi_0(y) = \left(\frac{e^{-\omega t}}{sinh\beta_3 h_\alpha}\right) sinh\beta_3 y \tag{3.16}$$

Substituting equation (3.16) into equation (3.10), we have:

$$\phi(y,t) = \left(\frac{sinh\beta_3 y}{sinh\beta_3 h_\alpha}\right) \tag{3.17}$$

Substituting equation (3.16) into equation (3.11), we have:

$$\frac{d^2\theta_0}{dy^2} + \beta_2^2\theta_0 = -\left(\frac{Rd_2 e^{-\omega t}}{sinh\beta_3 h_\alpha}\right) sinh\beta_3 y \tag{3.18}$$

Simplifying equation (3.20), we have:

$$\frac{d^2\theta_0}{dy^2} + \beta_2^2\theta_0 = \beta_4 sinh\beta_3 y \tag{3.19}$$

where $\beta_4 = -\left(\dfrac{Rd_2 e^{-\omega t}}{sinh\beta_3 h_\alpha}\right)$

The particular part of equation (3.19 is:

$$\theta_{0p} = A\sinh\beta_3 y + B\cosh\beta_3 y \tag{3.20}$$

Differentiating equation (3.20) according to the order of equation (3.19), we have:

$$\frac{d^2\theta_{0p}}{dy^2} = A\beta_3^2\sinh\beta_3 y + B\beta_3^2\cosh\beta_3 y \tag{3.21}$$

Simplifying equations (3.21) and (3.19), we have:

$$A = \frac{\beta_4}{(\beta_3^2 + \beta_2^2)}, B = 0 \tag{3.22}$$

Substituting equation (3.22) into equation (3.20), we have:

$$\theta_{0p} = \frac{\beta_4}{(\beta_3^2 + \beta_2^2)}\sinh\beta_3 y \tag{3.23}$$

The general solution of equation (3.19), we have:

$$\theta_0 = c_3 sin\beta_2 y + c_4 cos\beta_2 y + \frac{\beta_4}{(\beta_3^2 + \beta_2^2)} sinh\beta_3 y \tag{3.24}$$

Solving for the constant coefficients in equation (3.24) using equation (3.13), we have:

$$\theta_0 = c_3 sin\beta_2 y + \frac{\beta_4}{\left(\beta_3^2 + \beta_2^2\right)} sinh\beta_3 y \tag{3.25}$$

Simplifying equation (3.25), we have:

$$c_3 = \frac{e^{-\omega t}}{sin\beta_2 h} - \frac{\beta_4 sinh\beta_3 h}{\left(\beta_3^2 + \beta_2^2\right) sin\beta_2 h} \tag{3.26}$$

Substituting equation (3.26) into equation (3.25), we have:

$$\theta_0 = \left(\frac{e^{-\omega t}}{sin\beta_2 h} - \frac{\beta_4 sinh\beta_3 h}{\left(\beta_3^2 + \beta_2^2\right) sin\beta_2 h} \right) sin\beta_2 y + \frac{\beta_4}{\left(\beta_3^2 + \beta_2^2\right)} sinh\beta_3 y \tag{3.27}$$

Simplifying equation (3.27), we have:

$$\theta_0 = c_3 sin\beta_2 y + \frac{\beta_4}{\left(\beta_3^2 + \beta_2^2\right)} sinh\beta_3 y \tag{3.28}$$

Substituting equation (3.28) into equation (3.13), we have:

$$\theta(y,t) = \left(c_3 sin\beta_2 y + \frac{\beta_4}{\left(\beta_3^2 + \beta_2^2\right)} sinh\beta_3 y \right) e^{\omega t} \tag{3.29}$$

Results

In this section, we shall perform numerical simulation of the analytically solution and the results are segmented into velocity profile, temperature profile, and concentration profile respectively.

Fluid Temperature

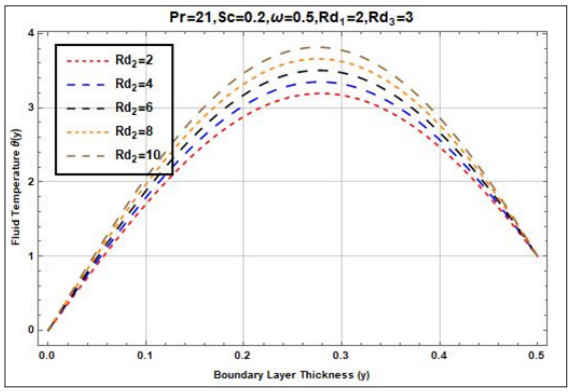

Figure 1: The Effect of Rate of Concentration on Fluid

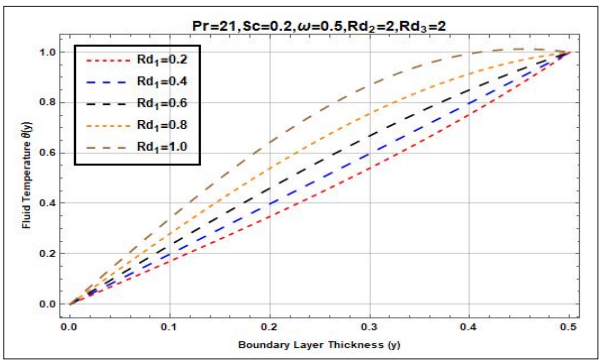

Figure 2: The Effect of Heat Source Change on FluidTemperature

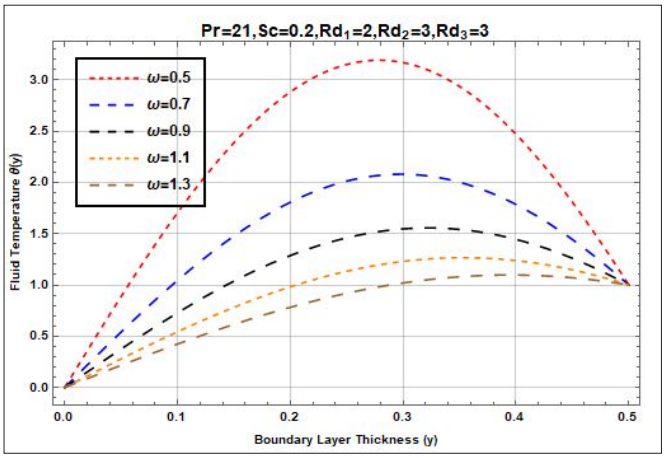

Figure 3: The Effect of Oscillatory Frequency on Fluid Temperature

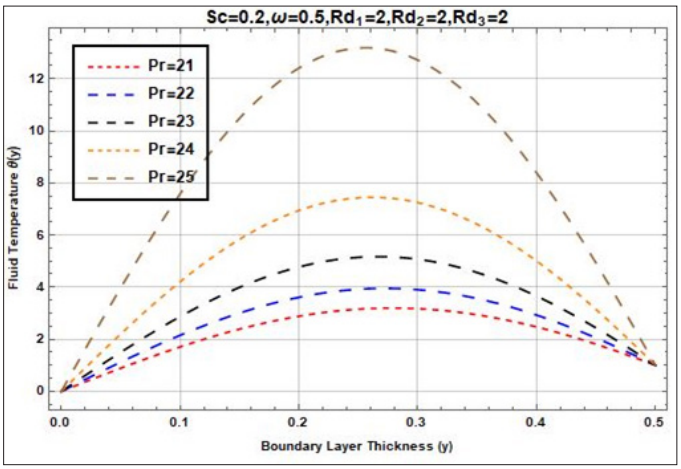

Figure 4: The Effect of Prandtl number on Fluid Temperature

Cell Mass Concentration

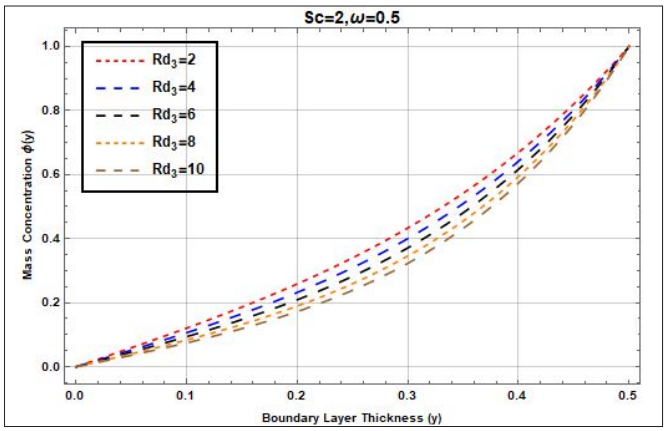

Figure 5: The Effect of Chemical Reaction on Cell Concentration

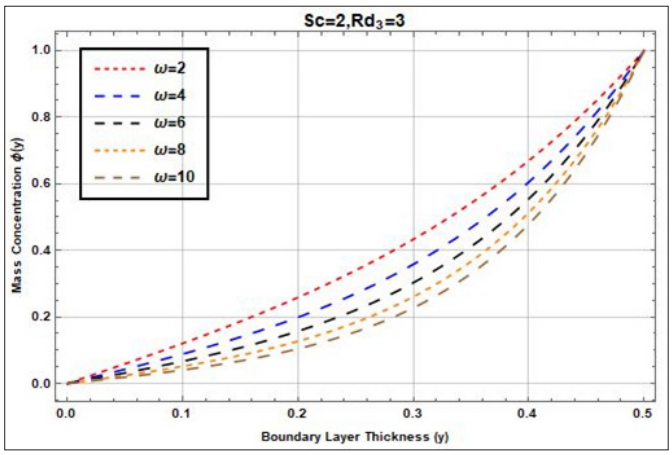

Figure 6: The Effect of Oscillatory Frequency on Cell Concentration

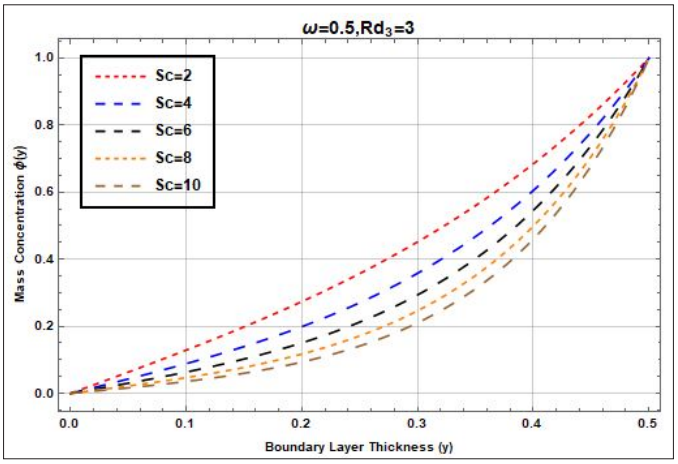

Figure 7: The Effect of Schmidt Number on Cell Concentration

Discussion of Result

In this section, we shall be discussing the analyzed results presented above. The results here involve the temperature and mass concentration profiles listed in Figure 1-8.

Figure 1 illustrates the effect of concentration rate on fluid temperature, and the result showed that the increasing concentration rate leads to higher temperature profiles. However, the concentration effects contribute to internal heat generation and it's very relevant in reactive biological and chemical systems, respectively. The effect of heat source change on fluid temperature was investigated, and the result is depicted in Figure 2, and the figure shows that stronger heat sources significantly raise fluid temperature as the thermal boundary layer thickness increases. The conclusion on that is that internal heat generation intensifies thermal energy storage. The study investigated the effect of oscillatory frequency on fluid temperature as illustrated in Figure 3. In addition, the figure elucidates that higher oscillatory frequency causes a decrease in temperature, which in turn enhances mixing and increases heat dissipation. Figure 4 illustrated the effect of the Prandtl number on fluid temperature, and it is seen that increasing the Prandtl number increases temperature near the wall. This is because the thermal boundary layer becomes thinner and the heat is retained close to the surface in high Prandtl fluid like blood.

Acknowledgment

We would like to acknowledge the Tertiary Education Trust Fund (TETFUND) for providing the needed funding to enable us to complete this research.

References

1. Daniel M, Szymanik Grzelak H, Sierdziński J, Podsiadly E, Kowalewska Mlot M et al. (2023) Epidemiology and risk factors of UTIs in children-A single-center observation. Journal of personalized medicine 13: 138-140.
2. Sahebkar A, Watts GF (2013) New LDL-cholesterol lowering therapies: pharmacology, clinical trials and relevance to acute coronary syndromes. Clinical therapeutics 35: 1082-1098.
3. Koter S (2002) Transport of simple electrolyte solutions through ion-exchange membranes-the capillary model. Journal of Membrane Science 206: 201-215.
4. Tziakas DN, Chalikias G, Pavlaki M, Kareli D, Gogi Raju R, et.al (2019) Lysed erythrocyte membranes promote vascular calcification: possible role of erythrocyte-derived nitric oxide. Circulation 139: 2032-2048.
5. Serjeant GR (2005) Mortality from sickle cell disease in Africa. BMJ 330: 432-433.
6. Makani J, Ofori Acquah SF, Nnodu O, Wonkam A, Ohene Frempong K (2013) Sickle cell disease: new opportunities and challenges in Africa. The scientific world journal 2013: 193-252.
7. Rees DC, Williams TN, Gladwin MT (2010) Sickle-cell disease. The Lancet 376: 2018-2031.
8. Balkaran B, Char G, Morris JS, Thomas PW, Serjeant BE, et al. (1992) Stroke in a cohort of patients with homozygous sickle cell disease. The Journal of pediatrics 120: 360-366.
9. Bunonyo KW, Ndu RI (2024) Mathematical Modelling and Numerical Simulation of Hematocrit and Pressure Effects on Blood Flow through Blood Vessel. International Research Journal of Pure and Applied Physics 11: 132-143.
10. Bunonyo KW, Dagana JT (2024) Mathematical Modelling of the Impact of Mass Concentration on Viscoelastic Fluid Flow through a Non-Porous Channel. Asian Journal of Pure and Applied Mathematics 6: 253-270.
11. Butter JK, Bunonyo KW, Eli IC (2024) Mathematical Modelling of the Thermosolutal Effect on Blood Flow through a Micro-Channel in the Presence of a Magnetic Field. British Journal of Multidisciplinary and Advanced Studies 5: 14-32.
12. Bunonyo KW, Ebiwareme L, Iworiso PB (2024) Mathematical modeling of time-dependent concentration of alcohol in the human bloodstream using the eigenvalue method. TWIST 19: 58-64.